Laboratory Studies of Spacecraft Fluid Lubricant Mobility and Film Thickness

Peter Frantz*, James Helt* and Steve Didziulis*

Abstract

Spacecraft mechanisms often rely upon very small amounts of lubricant to survive in the harsh conditions of space. In critical applications, thin oil films must provide both low drag and longevity, with ball bearings in some devices lasting hundreds of billions of loaded mechanical cycles. Our lab has developed several unique test facilities to measure the physical properties of thin liquid lubricant films, and to monitor their performance in realistic bearing level tests, such as ball bearings operating up to 6000 rpm. To understand and optimize lubricant performance, our groups strategy is to correlate bearing level test data with the chemical-physical properties of the lubricant and counter-body interfaces as they evolve during operation. This talk will provide an overview of our capabilities and highlight some unique aspects of thin film rheology and additive function.

Introduction

During the acquisition phase of spacecraft mechanisms, we are often asked to estimate the assets usable lifetime. Similarly, during operation we are asked to assist with extending mechanism life by critically assessing telemetry data that informs to the state of the lubricant. In both cases, mechanism life is usually determined by the life of the lubricant in the critical rolling and sliding interfaces. Once the lubricant is depleted, friction and wear lead to deteriorating performance and failure. This separates space mechanisms from many terrestrial applications, where lubricant may often be reapplied until failure occurs by other processes, such as rolling contact metal fatigue. For spacecraft mechanisms, retention of lubricant is of paramount importance.

When managing these mechanisms during operations, we periodically estimate the relative quantity of oil to monitor component health. Bearing drag torque, which is typically proportional to spin motor current, can be separated into three terms: 1) a “Coulombic” term, due to sliding and interfacial slip, 2) a hysteresis term, due to losses in compression of the Hertzian contact, and 3) a viscous term, due to displacement of the lubricant in the ball path. This final term, the viscous drag torque, has been shown to scale with viscosity to the 2/3 power[1]. Viscosity decreases with increasing temperature according to a model with functional form similar to the Arrhenius Equation[2, 3]. Taken together, over small changes in temperature, we find that the dependence of viscous drag on temperature is approximately linear, with the constant of proportionality referred to as the viscous coefficient (Q). This value is used as a relative measure of the lubricant in the critical interfaces of a spinning bearing. It is usually large at beginning of life, and tends towards zero late in life. Thus, it can be used as an indicator of bearing health.

When monitoring this value in a large population of similar high-speed mechanisms, we have found that (after lubricant run in) the value remains nearly constant for most of life. As the lubricant is depleted, the value gradually falls to zero. If there are two bearings in the component, we find that Q initially falls to half of its saturation value, and then later falls to near zero. A graphic representation of this process is shown in Figure 1 for a typical mechanism. For the first 14 years of operation of this hypothetical mechanism, the viscous coefficient (Q) hovered around 0.2 mA/°F. During the 7^{h} year, the Q value fell to approximately 0.1 mA/°F, and three years later it fell to near zero. At that point, retainer chatter and instability may begin to occur. The late stage behavior is interpreted as sequential starvation of the two bearings. The first one becoming depleted of oil at 7 years, indicated by the viscous drag falling to half of its original value. The

* The Aerospace Corporation, El Segundo, CA

second bearing was depleted at 10 years, where the viscous drag fell to near zero. After the onset of depletion sporadic relubrication events occur due to increased bearing disturbances and temperature.

Perhaps the most interesting observation of Figure 1, however, is the relative stability through most of life. Models of lubricant degradation and loss typically imply gradual consumption of oil, yet our observations show a stable quantity at the rolling and sliding interfaces until rapid loss late in life. This trend in Q is interpreted as being due to our imperceptibility of the total amount of lubricant in the bearing, much of which is not actively engaged in the critical interfaces. While this bulk oil is gradually consumed or lost, the oil in the interfaces is maintained at a constant level that is controlled by the combination of mechanical and surface forces acting on the oil. These forces are assumed to be constant during spacecraft operations, so the prevailing thought is that the oil volume does not change and is sustained in balance with oil reserves resting outside the active tribological interfaces. For example, this may be in the form of grease reserves that are channeled to the sides of the ball path.

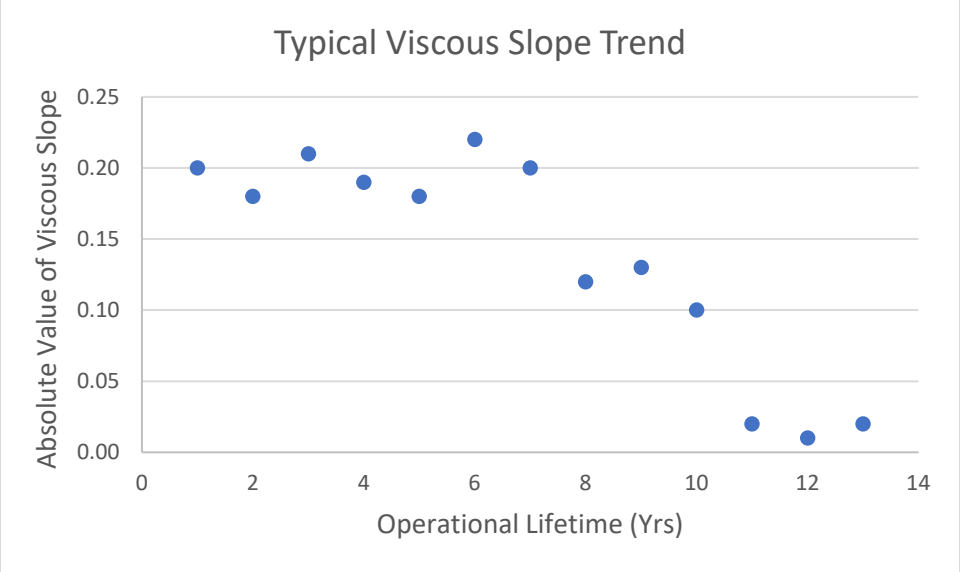

Figure 1. A graphic representation of the trends in viscous coefficient that are often observed in high-speed spinning devices.

A simplified model of the geometry is shown in Figure 2. The Hertzian contact between the ball and the race creates a capillary, which draws oil into a meniscus. At some distance from the contact are reserves of oil (held in grease thickener), and this oil migrates between these two bodies by creeping in a thin film across the bearing surfaces (balls, races, retainer). In addition to the capillary forces of the two bodies, the oil will be subject to mechanical forces (such as centrifugal acceleration) and other surface forces (such as thermocapillarity due to temperature gradients from localized heating). The direction and magnitude of lubricant creep will depend on the balance of these forces.

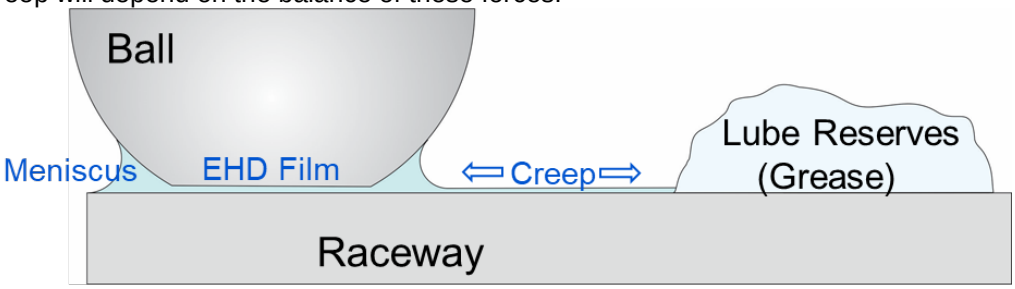

Figure 2. Schematic of an idealized ball/race contact and its relationship with lubricant reserves

This demonstrates that the sustenance of lubricant in the critical interfaces depends on lubricant mobility on bearing component surfaces. Ultimately, the longevity of critical spacecraft components depends on management of thin films of oil. Understanding the factors controlling these films is essential to prolonging life and responding to flight anomalies caused by lubricant starvation.

Thin Film Flow

The apparatus shown in Figure 3A is an adaptation of a device that has been described elsewhere to measure flow of very thin lubricant films[4-10]. In our work, the substrate is a polished steel coupon, with characteristics (composition, roughness, etc.) that are similar to bearing components. After a thin oil film (h < 5um) is cast onto a polished steel surface, a jet of nitrogen gas is then directed to the coupon surface causing the oil film to thin over time. Figure 3B shows an optical image of the film during thinning by the N_2 gas jet, where the fluids film thickness (h) is continuously monitored with an interferometer down to h ~10nm. The rate at which h declines over time, known as the thinning coefficient (β, units of nm*s), is proportional to the oil's viscosity and enables us to determine the viscosity of thin fluid films, a fundamental property that governs the oil's interfacial-surface mobility.

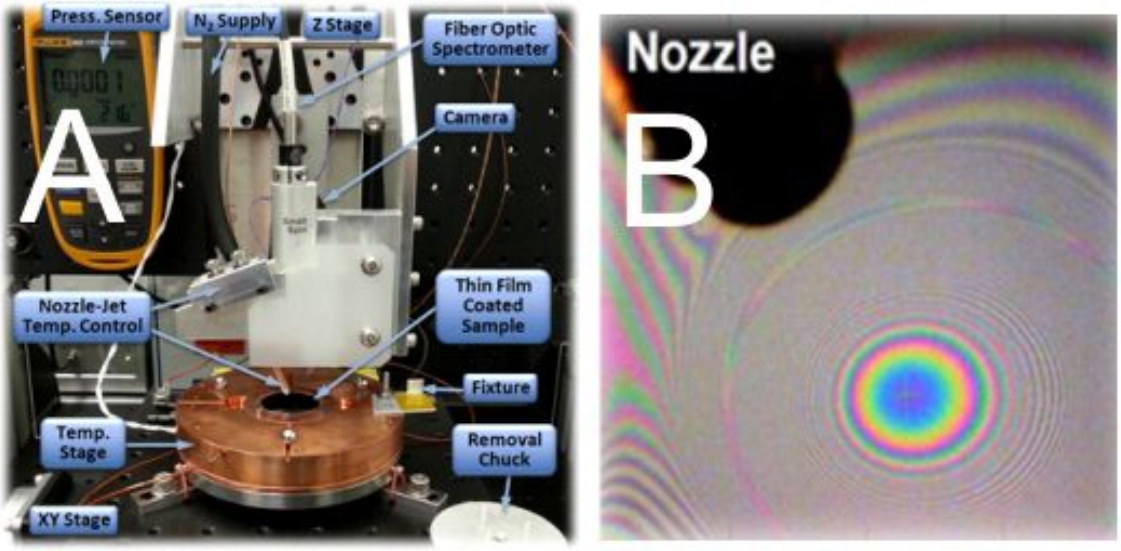

Figure 3. A) Thin Film Flow (TFF) apparatus, B) Thin film interference pattern after blow-off with a jet of nitrogen gas in the TFF.

Figure 4 shows an example of the film thickness (h) vs time during flow from the center of the target area. In this case, the sample was a 2-μm-thick film of a multiply-alkylated cyclopentane fluid. We find a rapid decrease in film thickness, with a functional form that appears similar to the film height decreasing in inverse proportionality to the elapsed time of exposure to the nitrogen jet. Figure 5 is the same data, plotted as the inverse film thickness ($1/h$) vs time. This plot provides a better demonstration of the inverse proportionality, where the slope is the thinning coefficient, β. We also find that there are two distinct regimes of viscous behavior. The first, with larger film thicknesses and early time of the experiment, represents the bulk properties of the fluid. The second regime represents the interfacial properties of the thin film, where interfacial forces that exist between lubricant molecules and the steel surface influence fluid mobility. In this case, the transition between these two regimes occurs at a film thickness of ca. 45 nm. After the transition to the interfacial regime, the viscosity was observed to increase by approximately 32%.

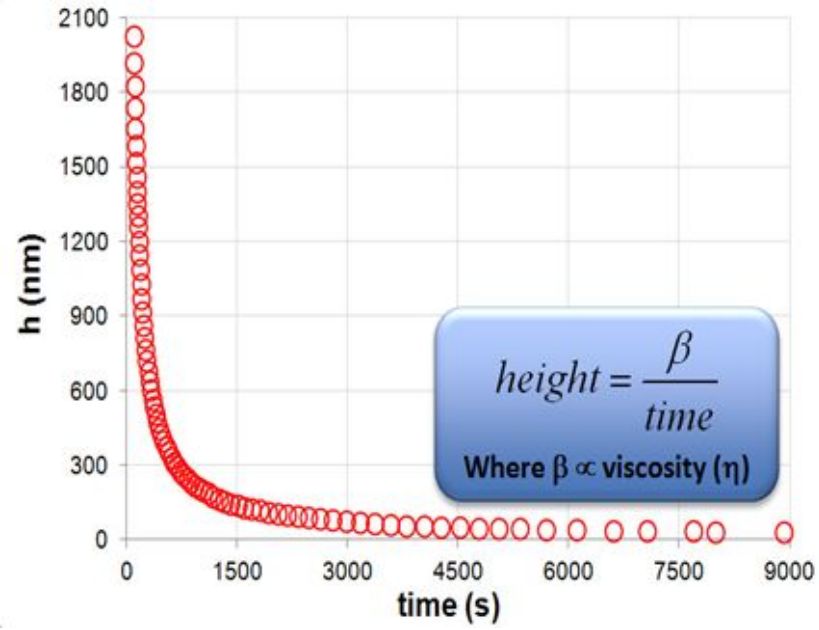

Figure 4. Plot of film oil film thickness vs time during blow-off using the TFF

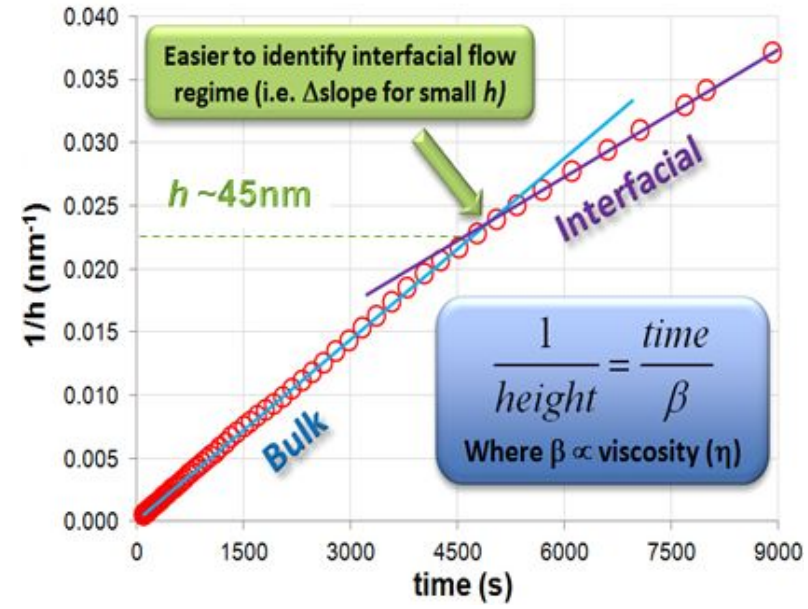

Figure 5. Plot of the data shown in Figure 4, using reciprocal of film thickness on the y-axis to show the inverse proportionality with time

These changes in viscosity and flow rate are important, because the process of resupply to the tribological contacts may be slowed as lubricant consumption proceeds and the scarcity of free oil leads to reduced oil film thicknesses.

Tribometry and Viscosity of Worn Lubricant Films

Another significant reduction in oil mobility during operational use may be caused by changes in oil composition. As the lubricant is worn in a tribological contact due to mechanical stresses and chemical reactions, some molecules are broken into smaller components while others are polymerized into larger

molecular weight varieties. The lower molecular weight products may evaporate more readily, and the larger products tend to accumulate in the vicinity of the contacts. This occurs with potential increases in the effective viscosity, and may affect both resupply of the contact and elasto-hydrodynamic film thickness. To study the effects of lubricant degradation and changing composition on surface flow in the contact region, we have mechanically worn the lubricant using a ball on disk tribometer in a vacuum chamber. This in-house developed instrument, shown in Figure 6, uses steel coupons similar to those shown above [7, 9, 11]. A multiply-alkylated cyclopentane oil with phosphate additives was used at 24°C and background pressure of 5 x 10^{-6} torr. With a load of 2.6 N, the contact stress was approximately 580 MPa and the diameter of the Hertzian contact area was 0.6 mm. The rotational speed was 90 rpm (boundary conditions). However, in some cases, a lateral oscillation was applied to lift the contact into EHD conditions.

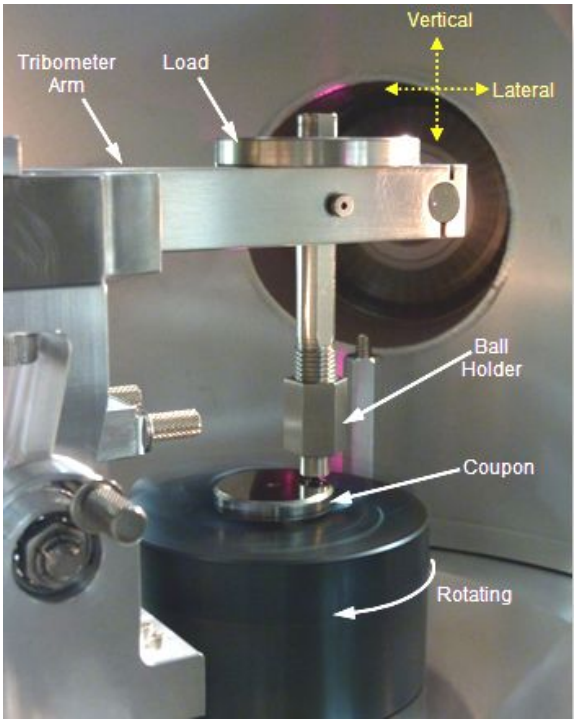

Figure 6. High vacuum ball-on-disk tribometer

After running under vacuum for 30 hr, samples were transferred to the TFF apparatus for measurements of viscosity. Three separate tests are shown in the top of Figure 7. The first two (Un88 and Un89) were performed at low speed, and Un 90 at high speed. In each case the contact path is visible as a distinct line in the oil film, caused by a defect in the otherwise gradual topography of the film thickness due to pinning and scalloping.

After blowing with nitrogen gas for over 1 hour, the displaced oil film patterns are shown in the bottom of Figure 7. In the two low speed examples, we find distinct regions of impeded oil flow that range from 3.1 to 5.2 mm across. These tracks are much larger than the diameter of the Hertzian contact, so they are not caused by changes in the substrate surface roughness. Instead they are related to the size of the ball/flat meniscus, where products of the lubricant degradation have been carried from the Hertzian contact and deposited in the region of oil reflow. In the high-speed case (Un90), bands of impeded oil flow are not easily detected and is likely because the EHD contact was not sufficiently stressful on the lubricant to create substantial wear and lubricant degradation polymerization products.

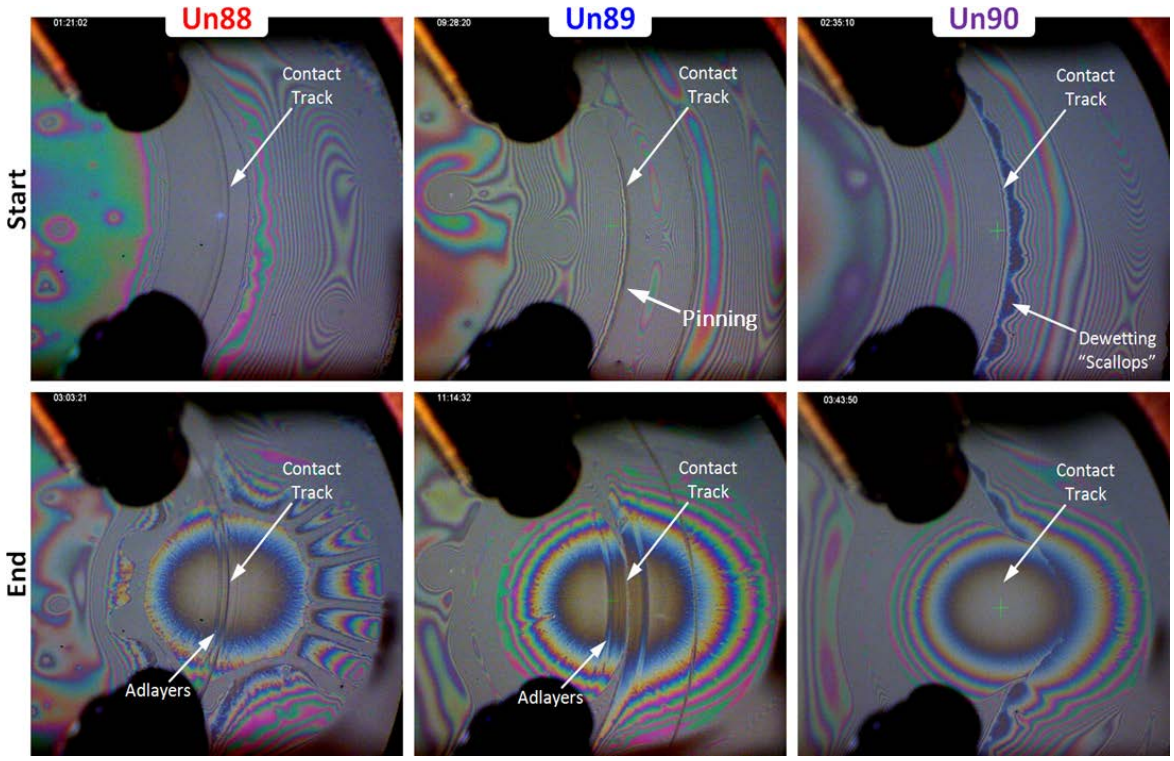

Figure 7. TFF measurements of oil mobility after wear in the high vacuum tribometer

During the thinning experiments shown in Figure 7, the film thickness was monitored interferometrically and plotted in Figure 8. Here, we compare the unworn base oil (green diamonds) with the low speed (red triangles and blue circles) and high speed (purple squares) test results. The results after the high-speed tests are within the experimental uncertainty of the unworn base oil tests. There are no detectable effects of running under EHD conditions for the times and pressures that were used. However, the impeded flow after the boundary tests are clearly seen in the lower slope (higher viscosity). Another distinguishing feature is that the slope continued to decrease as the film thickness reduced further in the later portions of the test. This implies that viscosity continued to increase with reduced thickness. Another observation is that the onset of interfacial flow increased from 100 nm with the unworn film to over 180 nm after low-speed testing and is due to the presence of much larger molecular weight species formed during degradation-polymerization.

Figure 9 provides a helpful visualization of the distribution of worn lubricant products in the vicinity of the contact. The image on the left shows the contact spot on the ball after testing, and the image on the right shows the sliding contact band on the coupon disk. The Hertzian contact spot, the zone of intimate contact between the ball and flat is at the center of the ring on the left-hand image. The “butterfly wing” lobes are caused by residue in the path of oil flow due to compression of the oil film on the surfaces and distortion of the oil meniscus caused by the dynamics of the sliding contact. The inlet zone of the contact is to the right, and the outlet is on the left. The reflow of oil in this pattern with each ball pass on the disk causes wear products to be swept from the Hertzian contact zone and deposited throughout the area covered by the base of the meniscus on the flat and the cap of the meniscus on the ball (details below). This results in adlayers of polymerized lubricant in the areas where oil flow is necessary for resupply of oil to the contact. Deposits of polymeric residue may impede flow of oil to the contact, reducing the volume of oil in the inlet zone, resulting in reduced EHD film thickness.

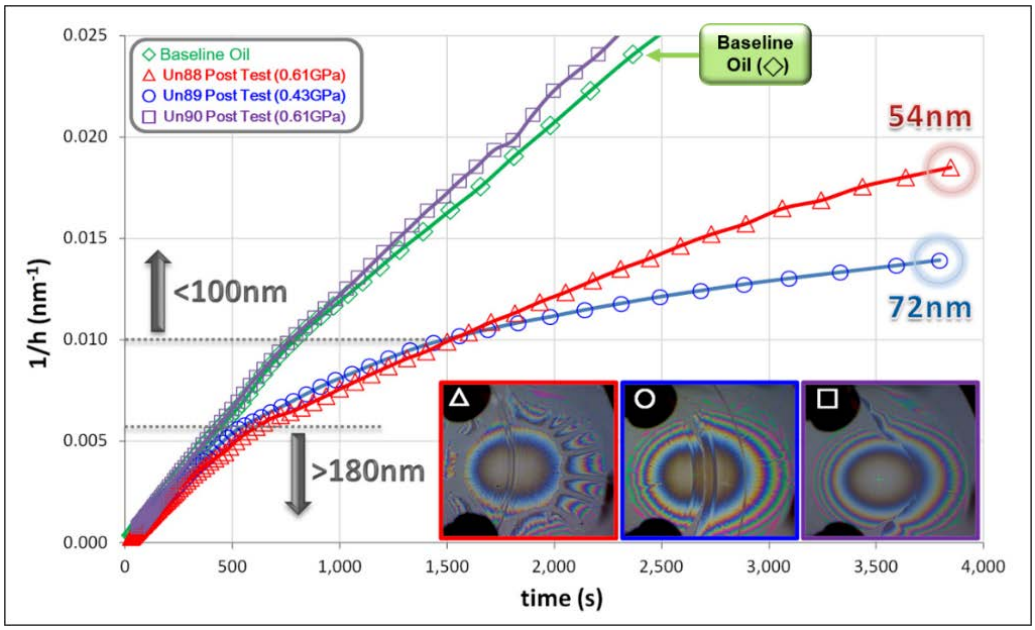

Figure 8. Results from measurements of oil mobility after wear in the high vacuum tribometer

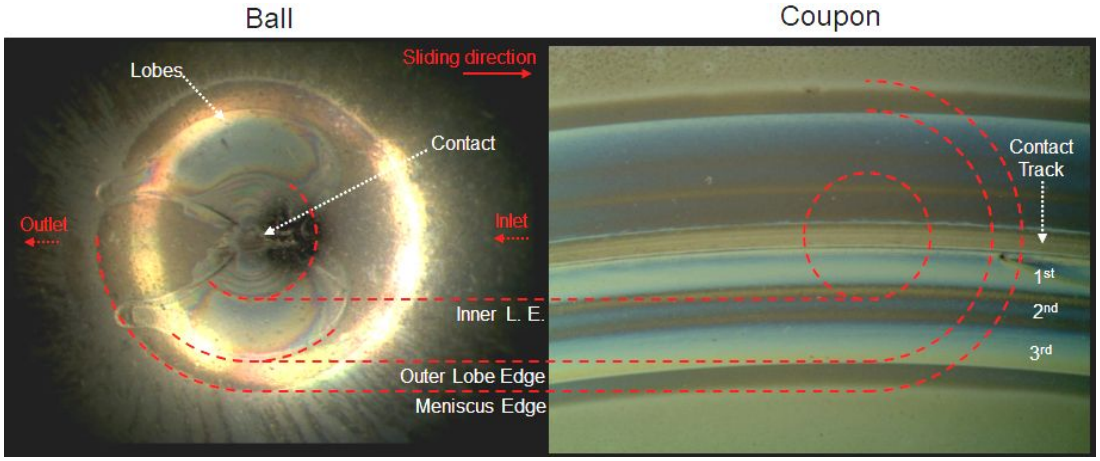

Figure 9. Optical micrographs of the ball and coupon surfaces after wear in the tribometer, showing patterns of lubricant wear product deposition

Film Stability and Wetting Tests

Resupply of oil to the active tribological contacts also depends on the stability and wettability of the fluid on the substrate. These, too, can depend on composition and film thickness. Thin film stability tests have been done to quantitatively evaluate *wetting* versus *dewetting* behavior by monitoring static evolution of a thin fluid film (h ~3 µm) deposited on a surface (e.g. 440C, 52100, SiOx). This is highly instructive for multi-component systems, such as formulated Pennzane oils, where additives can have an interfacial preference and modify the interfacial landscape ($\gamma_{sl,}$ the surface tension at the solid/liquid interface).

Each wetting test was conducted on two oxygen plasma cleaned 440C steel coupons[10]. Each test fluid was drop cast onto a coupon at room temperature. The fluids were cast from 100 µl of heptane solution that was diluted to 2.5% by volume. The drop cast technique preserves the test fluid stoichiometry and enhances diffusion for a uniform film that is close to its thermodynamically equilibrium state. Once applied,

the coupon is covered with a petri dish to allow time for stabilization. After 15 minutes, the dish is removed to allow the solvent to evaporate. Two photos are then acquired every 15 minutes with the coupon at room temperature. The coupon is then placed on a hot plate at 40°C for 15 minutes and then photographed again.

Figure 10 shows time dependent results for three different lubricant component samples. The top row shows thin film stability of a phosphate additive commonly used in aerospace mechanisms. After 15 minutes, there are numerous localized regions of dewetting across the surface. This fluid does not maintain a stable fluid on clean 440C steel. The second row shows the time sequence of a thin film of unformulated MAC oil. Dewetting is initiated at the edges of the coupon at room temperature, and the film rapidly retracts at 40°C. A thin film of MAC oil, formulated with the phosphate additive, is shown in the third row. Here, we find that the film is stable at all temperatures that were tested. It is evident that the additives are essential to maintain a stable film of oil in the laboratory environment.

Test Fluid	Additives	Dewet @ 15mins?	Dewet @ 30mins?	Dewet @ 45mins? (15mins @ 40°C)
Phosphate Additive	-	Yes, Local 	Yes, Local 	Yes, Local 
MAC Oil Unformulated	Nye antioxidants No Anti-wear	Yes, Perimeter 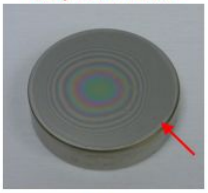	Yes, Perimeter 	Yes, Perimeter 
MAC Oil Formulated	Phosphate formulated (as received)	No 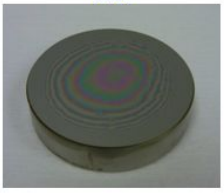	No 	No 

Figure 10. Photographs of steel coupons during oil wettability tests

Oil Meniscus Evolution

To help prolong the life of moving mechanisms, the lessons learned regarding mobility of lubricants must be ultimately applied to models of the supply rate of oil to the ball/race interface. The ultimate objective is to devise and test strategies for sustaining oil and promoting oil resupply at the critical ball/race interfaces. These efforts are guided by a theoretical model of oil uptake from the surrounding surfaces. As oil is drawn into the meniscus via surface tension and capillary forces, it fills the volume defined by a cylindrically symmetric annulus, with measurable base (b), waist, and cap (a) radii. A time interval optical microscopic imaging system was constructed to record images of a physical contact while the oil is flooding the meniscus.[8, 12] This system enables dynamic volume measurements over long periods of time. A screenshot of the meniscus analysis system is shown in Figure 11. Here, the meniscus profile, meniscus

volume and other elements describing the meniscus geometry are extracted and measured from optical images.

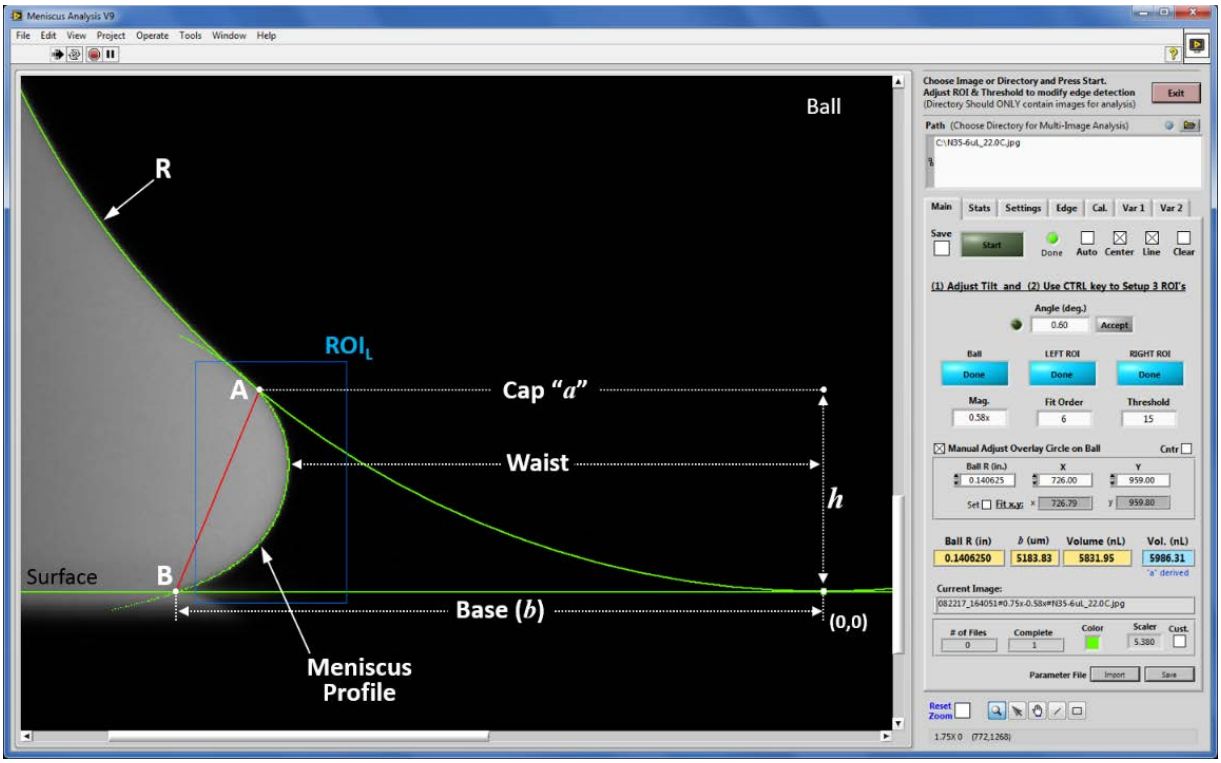

Figure 11. Screenshot showing the imaging window in a home-made application to measure the uptake of oil in the meniscus between a ball and flat.

An example of the evolution of these parameters during oil uptake in the meniscus is shown in Figure 12. In this case, the formulated MAC oil was cast as a thin film of 2.85 μm thickness on a clean 440C steel substrate at 25°C. A 440C ball was then brought into contact with the film at time t = 0, and the cap radius (a), meniscus height (h), and meniscus volume were monitored with time using the automatic imaging system. In this case, the meniscus growth was monitored for the first 180 hr and was only partially filled at that point. Each parameter was normalized to its value at 170 hr, so that they can be plotted together. We find continuous growth in volume that starts immediately upon contact, and is taken up at a rate that is controlled by thin film flow on the substrate and the changing capillary pressure as the ball/race interface floods.

Figure 13 shows the meniscus volume as a function of time, using a more viscous gyroscope oil. This series of tests was run until the volume saturated after approximately one day of uptake from a thin film. The data are compared against the results of a theoretical model which will be described elsewhere.

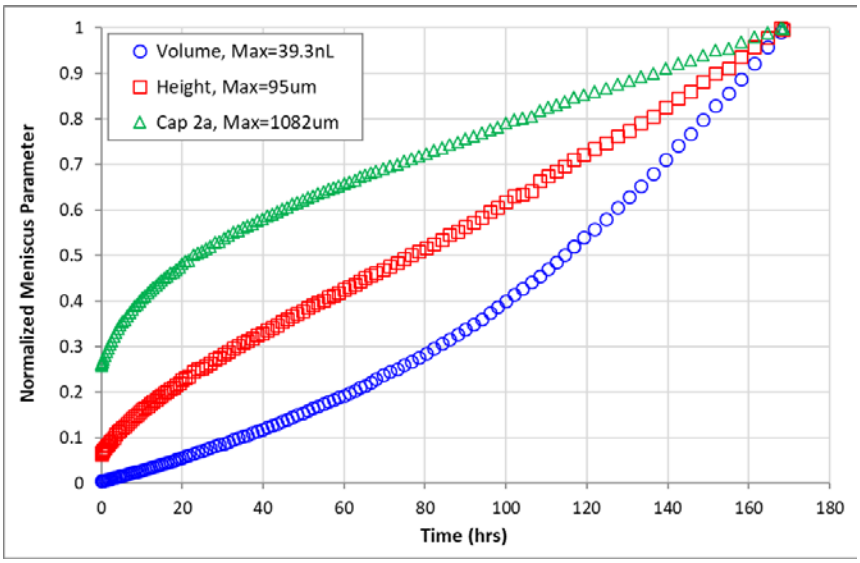

Figure 12. Three different geometric parameters of an MAC oil meniscus are shown as the capillary between a ball and flat is flooded with oil from a thin film on the flat

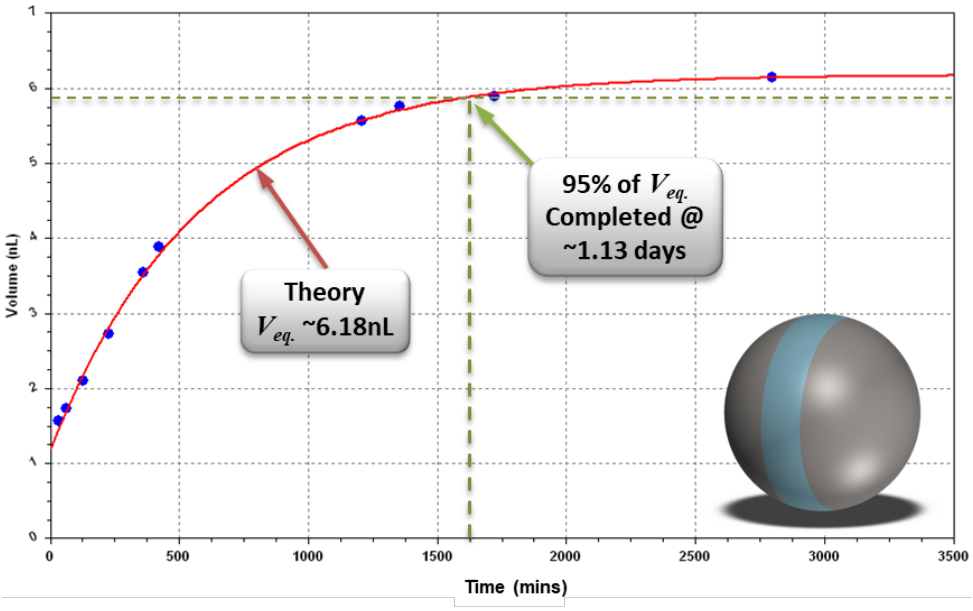

Figure 13. Time evolution of a ball/flat oil meniscus flooded by a thin film on the flat substrate

Effects of Composition on Oil Film Thickness

Changes in oil composition and mobility can ultimately affect the thickness and starvation of a protective oil film in the rolling contacts of high-speed bearings. The results above show the effective increase in viscosity of oil in the vicinity of a tribological contact due to polymerization. These results show the effects of changes in mobility due to deposition of lubricant degradation products, and illustrates that these products remain in the active tribological contacts. This would alter the molecular weight distribution as the mechanism ages, skewing it to heavier molecules and higher effective viscosity. To study the potential effects of aging on lubricant film thickness in spacecraft mechanisms, we have conducted EHD film thickness measurements on operating angular contact bearings using lubricants of similar chemical constituents and various molecular weights.

Film thickness measurements were performed using a device that has been described elsewhere [13-16]. Two angular contact bearings are mounted in a spring preloaded DF arrangement. As the EHD film thickness increases with speed, the resulting deflection of the outer rings is measured with capacitance proximity sensors. This displacement is simultaneously determined from changes in the dynamic preload using a load cell placed in series with the bearing preload. Figure 14 shows a schematic representation of the bearing deflection resulting from film thickness growth. At low speed, the balls are in intimate contact with the raceway surfaces. At high speed, the growth of the EHD film alters the bearing geometry, displacing the outer race to the right, and reducing the contact angle from b_1 to b_2. The change in film thickness is inferred from the outer ring displacement using a geometric model that represents the film thickness as an effective change in the ball diameter from d_1 to d_2. The change in contact angle is determined by measuring changes in the ball group frequency with respect to the shaft speed.

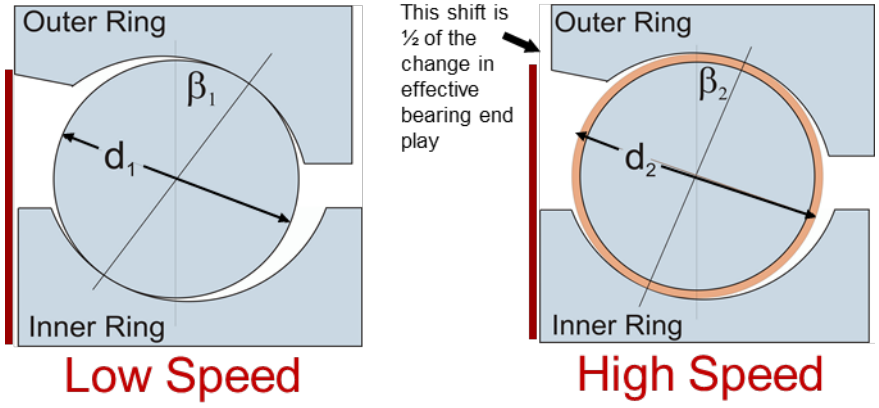

Figure 14. Cross section of an angular contact bearing at low and high speeds, showing effects of increasing EHD film thickness, modeled as an effective increase in ball diameter

Tests were conducted using poly alpha olefin samples of various viscosity. These lubricants were chosen due to their relevance to aerospace applications, their availability with different viscosities, and their simple composition compared to refined mineral oils. The oil samples were not formulated with additives. A small amount of oil was applied to bearings by first impregnating the retainers, and then centrifuging the retainer to remove bulk oil from the surface. The metal parts were coated with a thin film by solvent casting from a 10% solution of oil in heptane solvent.

After running-in the lubricant at 3000 rpm for 500 hours at room temperature, film thickness vs speed profiles were collected. These experiments were conducted by operating the bearings at a chosen speed, and then quickly stopping the shaft to collapse the film. The resulting rapid change in outer ring position was recorded and converted to oil film thickness using our geometric relationship. By measuring an instantaneous change in position, we avoid effects of thermal relaxation on the bearing structure that would otherwise overwhelm and obscure changes in the oil film thickness. This process was repeated after sequential increases in shaft speed from 60 to 3000 rpm.

An example of our results is shown in Figure 15, where EHD film thickness of two different PAO oils is plotted against speed from 60 to 3000 rpm. Orange circles are results from tests with a low viscosity PAO (10 cS at 100°C), and blue circles are from a more viscous oil (40 cS at 100°C). Tests were done with the bearings at 30°C. We find that the PAO40 film thickness increases much more rapidly with speed than the PAO10, as expected by theoretical estimates based on the Hamrock Dowson film thickness model.[17, 18] The more interesting observation, however, is the deviation from this model at high speeds due to kinematic starvation of the rolling contact.[19] We find that in this case the onset of starvation occurs at an approximately 600 rpm for the PAO40 and 900 for the PAO10. The difference is likely due to the reduced

mobility of the more viscous oil, impeding the reflow of oil from the periphery of the contact back into the inlet zone. These results show the degree to which film thickness depends on viscosity.

As lubricant deteriorates in an aging satellite mechanism, we may expect similar increases in film thickness. However, the experiments shown here were performed after only 500 hours of operation. While this is enough time for run-in of the lubricant and stabilization of the film thickness, it is not sufficiently long to reach the more severely starved conditions of a late-life satellite mechanism. For that reason, we suspect these film thicknesses are not representative of such conditions. Future experiments will explore the effects of lubricant depletion.

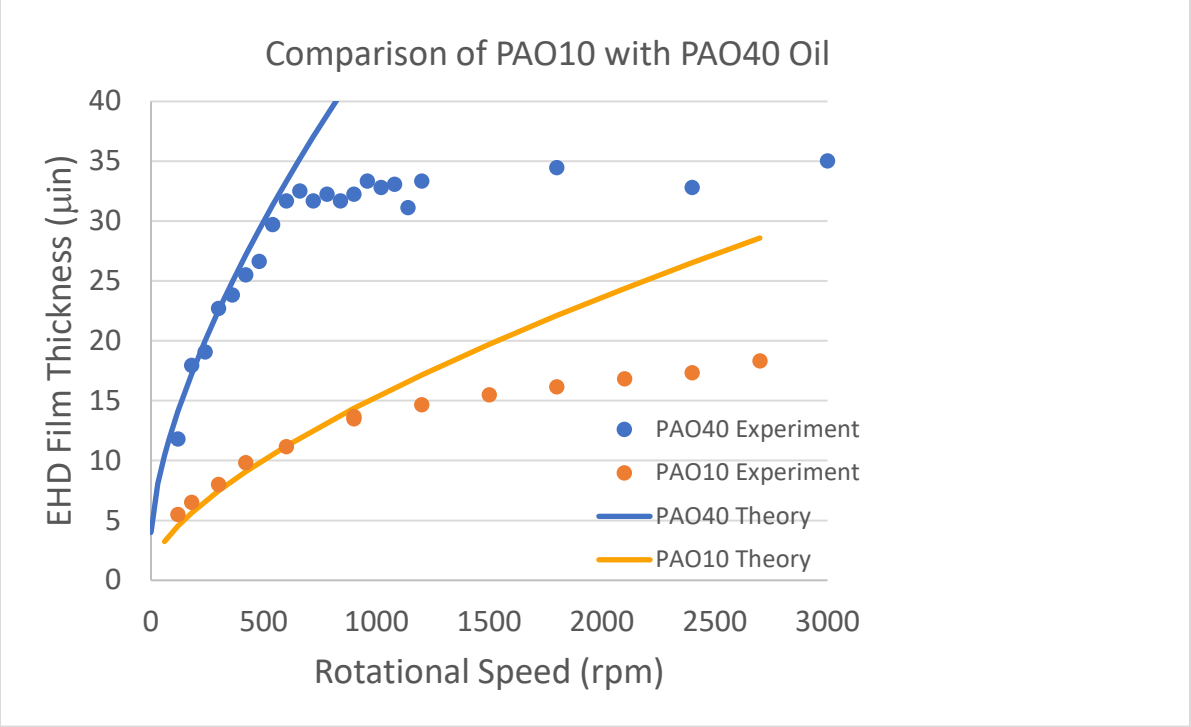

Figure 15. Dependence of EHD film thickness on speed, for two lubricants with similar chemistry and molecular architecture, but different molecular weight and viscosity. Circles are experimental measurements; solid lines are fits to Hamrock-Dowson model

Conclusions

Lubrication is an essential component of any moving mechanical assembly. In most space mechanisms, where the lubricant cannot be easily replenished, degradation and loss of the oil ultimately leads to changes in performance and an end to component life. Our goals have been to develop a better understanding of how to manage those changes in performance and to delay the end of life. The experimental techniques and the selected results shown here demonstrate our approach to achieving these goals.

Among the lessons learned from this study are that: 1) Spacecraft component life often depends on management of thin films in an evolving environment, 2) Oil mobility decreases with film thickness, 3) Oil mobility decreases as it degrades in a tribological contact, 3) new techniques can detect subtle changes in lubricant composition, 4) these changes can affect wettability, mobility, and resupply of oil to critical contacts, and 5) impeded resupply can reduce the thickness and stability of a protective film between two surfaces.

References

1. Palmgren, A. and B. Snare, *Influence of Load and Motion on the Lubrication and Wear of Rolling Elements.* Inst. Of Mech. Eng., 1957. **79**: p. 454-458.
2. Helt, J.M., *Density, Dynamic and Kinematic Viscosity of Bearing Lubricating Oils and Additives*. 2019, The Aerospace Corporation: El Segundo, CA.
3. Messaâdi, A., et al., *A New Equation Relating the Viscosity Arrhenius Temperature and the Activation Energy for Some Newtonian Classical Solvents.* Journal of Chemistry, 2015. **2015**(3): p. 12 pages.
4. Deryagin, B.V. and V.V. Karasev, *The Study of the Boundary Viscosity of Organic Liquids by the Blow-off Method.* Russian Chemical Reviews, 1988. **57**(7): p. 634-647.
5. Scarpulla, M.A., C.M. Mate, and M.D. Carter, *Air shear driven flow of thin perfluoropolyether polymer films.* The Journal of Chemical Physics, 2003. **118**(7): p. 3368-3375.
6. Berendsen, C.W.J., et al., *Rupture of Thin Liquid Films Induced by Impinging Air-Jets.* Langmuir, 2012. **28**(26): p. 9977-9985.
7. Helt, J.M., *High-Vacuum Tribometry Tests of Fluid Lubricants on Bearing Steels*. 2013, The Aerospace Corporation: El Segundo, CA.
8. Helt, J.M. and P.F. Frantz, *Investigating the Reflow of Gyroscope Lubricant SRS160 on Bearing Surfaces: Analysis Methods and Techniques*. 2013, The Aerospace Corporation: El Segundo, CA.
9. Helt, J.M., *High vacuum tribometry tests of fluid lubricants on bearing steels*, in *ACS National Meeting*. 2014: San Francisco CA.
10. Helt, J.M., *Procedure for Separating Pennzane Oil from Formulated Oils and Rheolube Based Greases*. 2016, The Aerospace Corporation: El Segundo, CA.
11. Helt, J.M. and J.J. Kirsch, *High Vacuum Tribometer for Fluid Lubricated Bearing Material Testing: Part 1 – Instrument Design*. 2010, The Aerospace Corporation: El Segundo, CA.
12. Didziulis, S., J. Helt, and P. Frantz, *Laboratory Studies of Spacecraft Fluid Lubricants*, in *ACS National Meeting*. 2019: San Diego CA.
13. Ward, P.C., A.R. Leveille, and P.P. Frantz, *Measuring the EHD Film Thickness in a Rotating Ball Bearing*, in *Proceedings of the 39th Aerospace Mechanisms Symposium*. 2008: NASA Marshall Space Flight Center.
14. Helt, J.M., *EHD Bearing Test Unit: Final Design*. 2016, The Aerospace Corporation: El Segundo, CA.
15. Helt, J.M., *EHD Bearing Test Unit: Setup & Operation Overview*. 2017, The Aerospace Corporation: El Segundo, CA.
16. Helt, J.M., *EHD Bearing Test Unit: Automated Test and Analysis Framework*. 2018, The Aerospace Corporation: El Segundo, CA.
17. Dowson, D. and G.R. Higginson, *Elasto-hydrodynamic lubrication the fundamentals of roller and gear lubrication.* 1966.
18. Hamrock, B.J. and D. Dowson, *Isothermal Elastohydrodynamic Lubrication of Point Contacts: Part III—Fully Flooded Results.* Journal of Tribology, 1977. **99**(2): p. 264-275.
19. Coy, J.J. and E.V. Zaretsky, *Some Limitations in Applying Classical EHD Film Thickness Formulas to a High-Speed Bearing.* Journal of Tribology, 1981. **103**(2): p. 295-301.